Superplastic Forming by Decomposition of ($CaCO_3$ + C) and $MgCO_3$

J.S. Shyu and T.H. Chuang

An innovative method has been developed that replaces argon as the pressure source for superplastic forming. In this new process, several solid materials are placed in a closed system to generate pressure and are capable of forming superplastic alloy plates at specific temperatures. In the present study, the total pressures for the decomposition of ($CaCO_3$ + C) and $MgCO_3$ have been theoretically calculated from thermodynamics. The results show that a pressure range of 40 to 396 psi can be obtained for the ($CaCO_3$ + C) system between 850 and 1000 °C, which is suitable for the superplastic forming of Ti-6Al-4V and Superdux 64 (Nippon Yakin Kogy Co., Ltd., San-ei Bridge, Kyobasi 1-5-8, Chyuoku, Tokyo 104, Japan) stainless steel. The pressure for $MgCO_3$ system between 480 and 515 °C ranges from 78 to 160 psi, which is suitable for the superplastic forming of 8090 Al-Li and 7475 Al-Zn-Mg alloys. The calculated temperature dependence of pressure is consistent with the experimentally measured results. Furthermore, the forming rates, wall thickness distributions, tensile properties, and microstructures of the four alloys after forming have been shown to be very similar to those of conventional superplastic forming by argon pressurization.

Keywords

decomposition, forming speed, internal pressure, post-forming speed, superplastic forming

1. Introduction

SUPERPLASTIC forming is most commonly accomplished by the "gas blowing" method (Ref 1, 2), which involves the use of expensive argon gas. This method requires pipelines, flow control valves, and an apparatus for generating pressure (Ref 3), all of which make designing the tooling and workpiece structure more difficult. To eliminate these disadvantages, an innovative method has been developed that uses reaction gases generated by the vaporization or decomposition of solid materials. This method can also be performed concurrently with diffusion bonding, brazing, or transient liquid-phase bonding to obtain complex metallic structures from a number of workpieces (Ref 4, 5) and can also be used to manufacture spherelike hollow bodies through a die-free method (Ref 6).

In the present study, the total pressures for decomposition of ($CaCO_3$ + C) and $MgCO_3$ have been theoretically calculated by using thermodynamics and have been compared with the experimental measurements. Furthermore, dome-shaped workpieces have been produced to confirm the applicability of this method. For this purpose, four commercial superplastic alloys (Ti-6Al-4V, Superdux 64 stainless steel, 8090 Al-Li, and 7475 Al-Zn-Mg) were employed. Also, tensile specimens were taken from the pan-shaped workpieces formed by this method to evaluate the mechanical properties of the materials after formation. Oxide scales formed on the surfaces of the workpieces and the resulting microhardness depth profiles have also been analyzed. Finally, the microstructures of the four superplastic alloys before and after forming have been compared.

J.S. Shyu and **T.H. Chuang,** Institute of Materials Science and Engineering, National Taiwan University, Taipei, Taiwan, R.O.C.

2. Theoretical Calculations of Internal Pressure

Carbon dioxide and carbon monoxide can be generated by mixing $CaCO_3$ and carbon powders in a closed system. By using thermodynamics (Ref 7), the total pressure of CO_2 and CO can be calculated by:

$$P_{\text{total (psi)}} = \left(P_{CO_2}\right)14.7 * \exp\left(17.32 - \frac{20254}{T}\right) + \left(P_{CO}\right)14.7 * \left[\exp\left(38.3 - \frac{40784.7}{T}\right)\right]^{0.5}$$

(1 atm = 14.7 psi)

For different temperatures, the total pressure calculated and the suitable alloy system are as listed in Table 1.

Table 1 Total pressures calculated for ($CaCO_3$ + C) in a closed system

Temperature °C	Temperature K	$P_{CO_2} + P_{CO} = P_{total}$, psi	Alloy system
850	1123	6 + 34 = 40	Ti-6Al-6V-2Sn
927	1200	23 + 128 = 151	Ti-6Al-4V
985	1258	50 + 278 = 328	Superdux 64
1000	1273	60 + 336 = 396	Superplastic Inconel 718

Table 2 CO_2 pressures calculated for decomposition of $MgCO_3$ in a closed system

Temperature °C	Temperature K	P_{CO_2}, psi	Alloy system
480	753	78	8090, 7475, and 5083 Al alloys
490	763	100	8090, 7475, and 5083 Al alloys
500	773	127	8090, 7475, and 5083 Al alloys
515	788	160	8090, 7475, and 5083 Al alloys

For the decomposition of $MgCO_3$, the CO_2 pressure can be calculated (Ref 7):

$$P_{CO_2\,(psi)} = 14.7 * \exp\left(20.45 - \frac{14144}{T}\right)$$

For different temperatures, the pressure calculated and the suitable alloy system are as listed in Table 2.

In fact, however, pure $MgCO_3$ is difficult to obtain. Its common form is $(MgCO_3)_4Mg(OH)_2{\cdot}xH_2O$, where $x = 1$ to 4 (basic magnesium carbonate), and the behavior of pressure varying with temperature may be similar to that of $MgCO_3$ but not completely identical.

The amount of powder needed can be calculated roughly by using the ideal gas equation.

3. Experimental Method

Four commercial superplastic alloys were used in this study: Ti-6Al-4V alloy, Superdux 64 stainless steel, 8090 Al-Li alloy, and 7475 Al-Zn-Mg alloy, with thicknesses of 1, 1, 1, and 1.6 mm, respectively. Their nominal compositions are given in Table 3.

To measure internal pressure, the tested powder used to generate the internal pressure was placed in a mold made of 310 stainless steel (Fig. 1). A thin type 316 stainless tube was connected to the mold, and at the other end of this tube was attached a pressure meter. The mold was sealed by using an oil press during heating and cooling. For $CaCO_3$ and carbon, the testing temperature was 1000 °C, and for $(MgCO_3)_4Mg(OH)_2{\cdot}xH_2O$ the temperature was 500 °C.

In order to confirm the applicability of this method, dome-shaped workpieces were produced (Fig. 2a). The forming rate and wall thickness of the specimens were measured.

To evaluate mechanical properties after formation, tensile specimens (12 mm gage length and 5 mm gage width) were taken from the pan-shaped workpieces (Fig. 2b), which were superplastically bulge formed into a cylindrical die with a diameter of 110 mm and a depth of 40 mm. The amount of superplastic strain that these workpieces had undergone was calculated as an equivalent tensile strain (ETS) using the relationship (Ref 8):

$$ETS\% = (S_0/S - 1) \times 100$$

where S_0 and S are the initial and final sheet thicknesses, respectively. During formation of the pan-shaped specimens, deformation was restricted at the pole when the free bulged dome touched the die. Deformation continued in regions not in contact with the die, and this led to a uniform thickness of the flat

Table 3 Nominal alloy compositions

Alloy	Nominal composition, wt %
Ti-6Al-4V	Ti-6.39Al-4.01V-0.16Fe-0.012N-0.018C-0.0018H-0.15O-0.001Y
Superdux 64	Fe-5.9Ni-23.8Cr-1.5Mo-0.03C-0.7Si-0.7Mn-0.035P-0.002S-1.1Cu-0.05Al-0.14N
8090	Al-1.09Cu-0.77Mg-0.02Si-0.05Fe-0.02Zn-0.026Ti-0.11Zr-2.38Li
7475	Al-1.54Cu-2.26Mg-0.04Si-0.07Fe-5.55Zn-0.02Ti-0.19Cr-0.01Mn

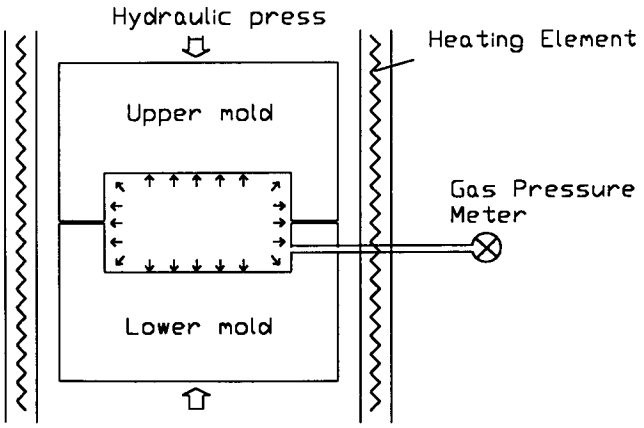

Fig. 1 Apparatus for measurement of internal pressure

(a)

(b)

Fig. 2 Typical dome-shaped (a) and pan-shaped (b) specimens formed by internal pressure for formability evaluation and tensile testing, respectively. (a) Ti-6Al-4V. (b) 8090 Al-Li

base of the pan-shaped specimen (although the thickness decreased markedly close to the corner of the die). Small variations in specimen thickness and any solute-deleted layers or oxide layers in the areas corresponding to the gage sections were removed by grinding. Tensile tests were carried out at a constant crosshead speed of 3 mm/min. Because of the obvious degradation of the mechanical properties of the aluminum alloys, the effect of post-heat treatment was also studied.

The oxide scale that formed on the specimens was examined by means of x-ray diffraction (XRD). Microstructures were examined by scanning electron microscopy (SEM), and microhardness on the cross sections was measured. For these purposes, samples were sectioned from the base of the pan-shaped workpieces and metallographically prepared for cross-sectional views.

4. Results and Discussion

The reaction gas pressure of the $CaCO_3$ powder mixed with carbon powders is shown in Fig. 3. The dashed line represents the result derived from theoretical calculations by thermodynamics. Curve A shows a low heating rate. (It took 250 min to heat from room temperature to 1000 °C.) Curve B shows the general heating rate of the experimental apparatus. (It took 55 min to heat from room temperature to 1000 °C.)

Figure 4 shows the gas pressure for the decomposition of $(MgCO_3)_4Mg(OH)_2{\cdot}xH_2O$ as it varied with temperature. Compared with the theoretical curve of $MgCO_3$, it can be seen that the decomposition reaction of $(MgCO_3)_4Mg(OH)_2{\cdot}xH_2O$ is more complicated than that of $MgCO_3$. During the formation of superplastic alloys using ($CaCO_3$ +

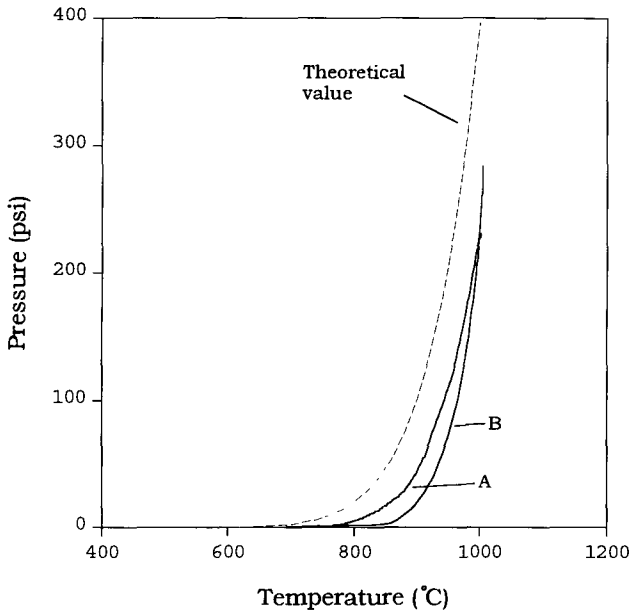

Fig. 3 Internal pressure of $CaCO_3$ and carbon powders versus temperature

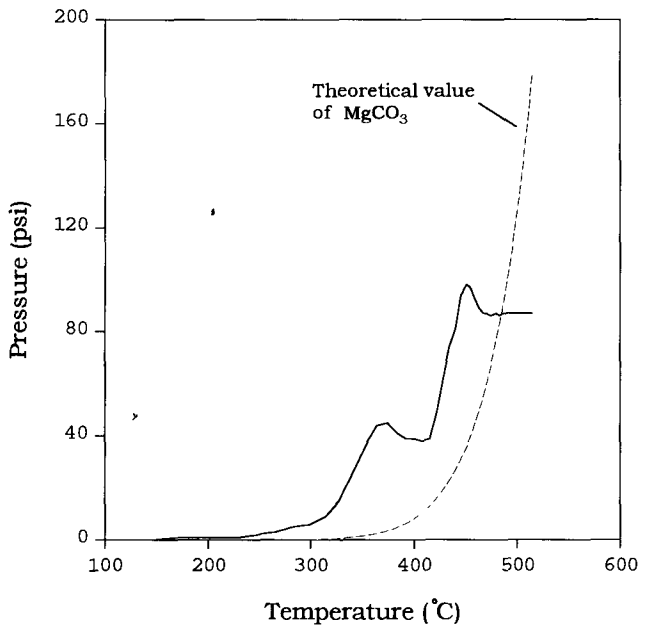

Fig. 4 Internal pressure of $(MgCO_3)_4Mg(OH)_2{\cdot}xH_2O$ powder versus temperature

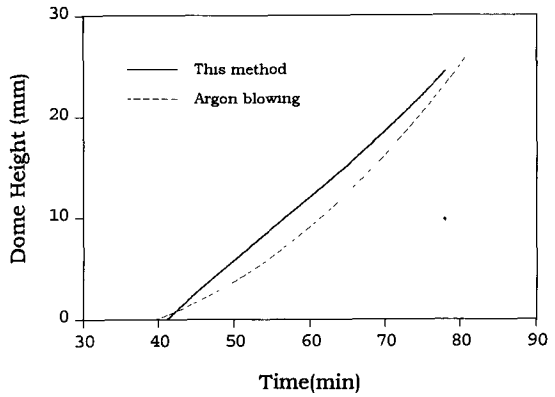

(a)

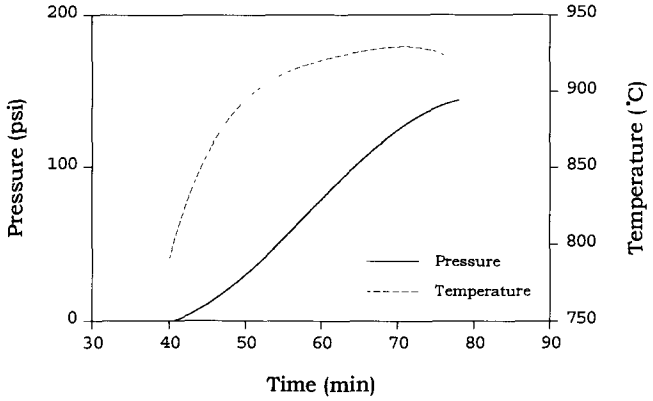

(b)

Fig. 5 Ti-6Al-4V. (a) Forming dome height versus heating time (forming radius of 25 mm). (b) Temperature and forming gas pressure versus heating time

C) or $(MgCO_3)_4Mg(OH)_2{\cdot}xH_2O$, deformation took place whenever the pressure was great enough, even though the temperature did not reach the optimal value.

Figure 5(a) shows the forming dome heights for Ti-6Al-4V alloy. The solid line represents the dome height derived using this method, and the dashed line represents that derived using the conventional argon blowing method, which followed the same pressure history of this method (Fig. 5b) during formation. Both of the forming speeds were identical no matter what kind of gas source was used. The wall thickness distributions of the dome-shaped specimen formed with internal pressure and argon are shown in Fig. 6. Both domes had nearly the same forming dome heights of about 25 mm. Comparison of the two curves shows that the difference is small.

Figure 7(a) shows the forming dome heights for Superdux 64 stainless steel. Comparison of the two curves derived using this method and using argon blowing, which followed the same pressure history (Fig. 7b) during formation shows both forming speeds to be almost the same. The wall thickness distributions of the dome-shaped specimens formed with internal pressure and argon are shown in Fig. 8. The difference is not obvious.

The forming heights and pressure/thermal history for 8090 Al-Li alloy are shown in Fig. 9(a) and (b), respectively. The specimen wall thickness distributions are shown in Fig. 10. Similar to Ti-6Al-4V and Superdux 64 stainless steel, both the forming speeds and the specimen wall thickness distributions using this method are close to those obtained by argon blowing following the same pressure history during formation.

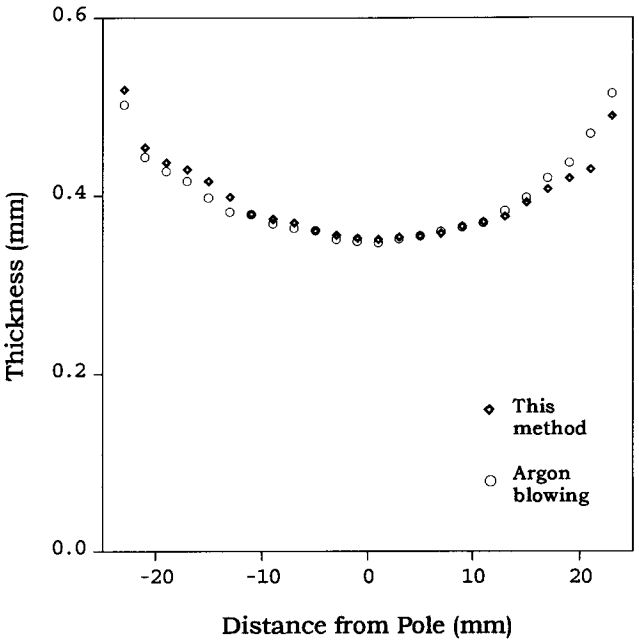

Fig. 6 Thickness distributions of the Ti-6Al-4V dome-shaped specimens formed with internal pressure (dome height of 24 mm) and argon (dome height of 23.7 mm)

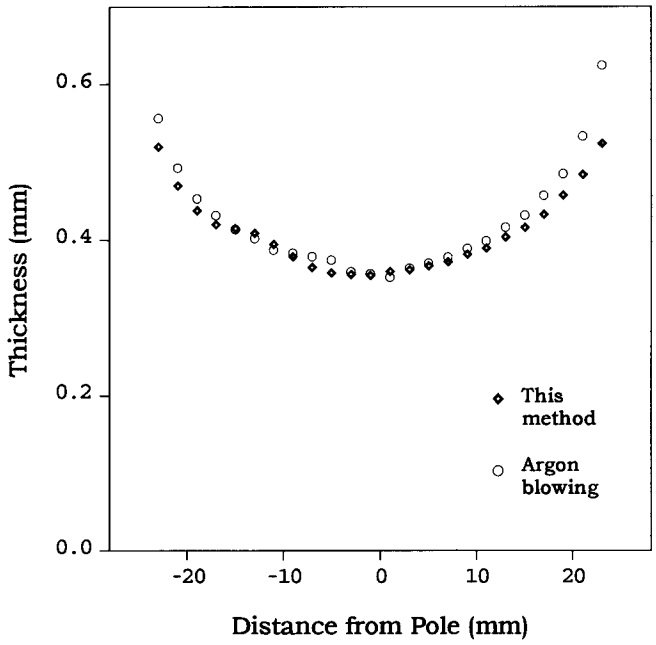

Fig. 8 Thickness distributions of the Superdux 64 stainless steel dome-shaped specimens formed with internal pressure (dome height of 28.3 mm) and argon (dome height of 27.5 mm)

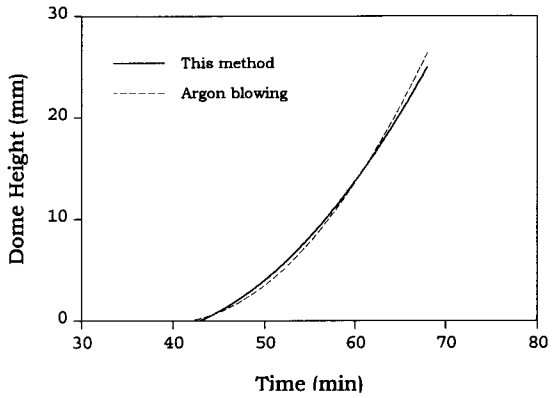

(a)

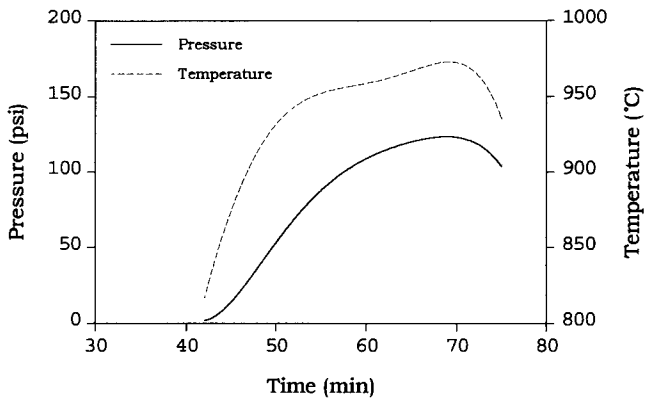

(b)

Fig. 7 Superdux 64 stainless steel. (a) Forming dome height versus heating time (forming radius of 25 mm). (b) Temperature and forming gas pressure versus heating time

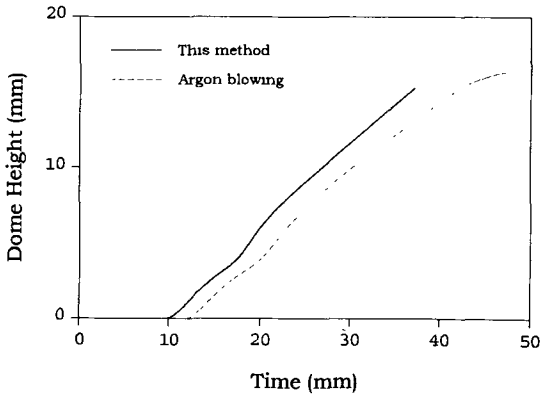

(a)

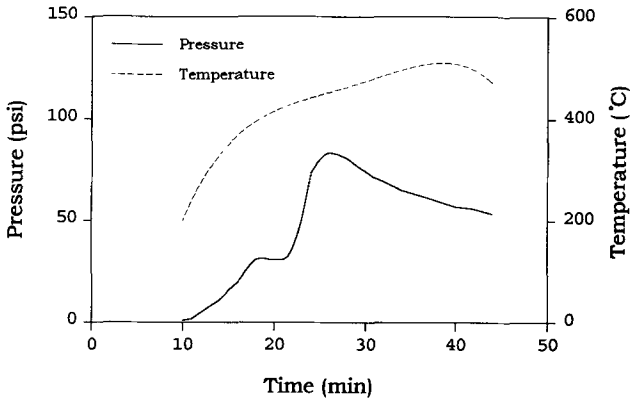

(b)

Fig. 9 8090 Al-Li alloy. (a) Forming dome height versus heating time (forming radius of 15 mm). (b) Temperature and forming gas pressure versus heating time

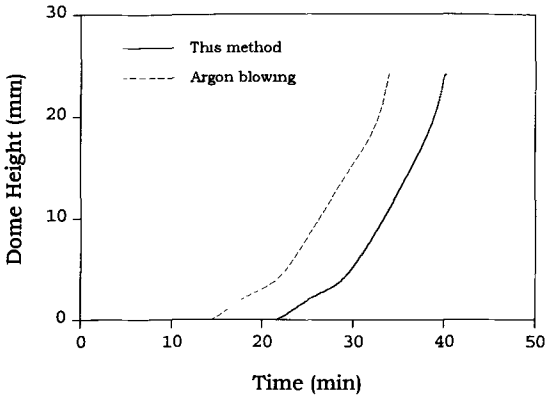

(a)

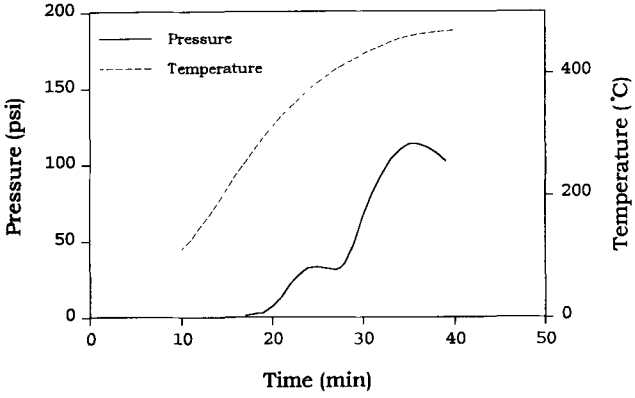

(b)

Fig. 11 7475 Al-Zn-Mg alloy. (a) Forming dome height versus heating time (forming radius of 25 mm). (b) Temperature and forming gas pressure versus heating time

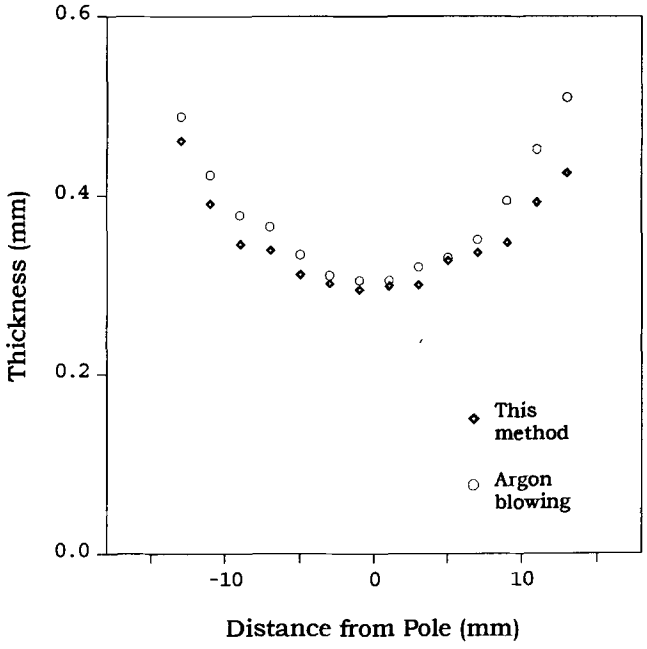

Fig. 10 Thickness distributions of the 8090 Al-Li alloy dome-shaped specimens formed with internal pressure (dome height of 16.1 mm) and argon (dome height of 15.5 mm)

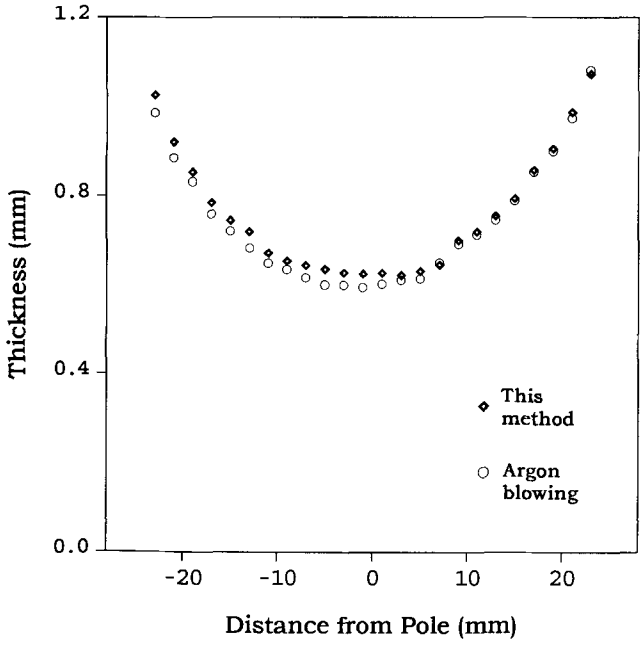

Fig. 12 Thickness distributions of the 7475 Al-Zn-Mg alloy dome-shaped specimens formed with internal pressure (dome height of 25.8 mm) and argon (dome height of 25.5 mm)

Table 4 Alloy tensile properties

Material	Test condition(a)	ETS, %	0.2% Proof stress, MPa	Tensile stress, MPa	Elongation, %
Ti-6Al-4V	A	...	925	1008	19
	B	80	840	940	14
	C	80	856	950	13
Superdux 64	A	...	560	977	26
	B	60	520	777	6
	C	60	505	732	5
8090	A	...	140	303	12
	B	60	146	282	12
	C	60	160	249	14
	A + T6	...	211	447	10
	B + T6	...	194	417	11
	C + T6	...	204	432	12
7475	A	...	469	543	16
	B	90	202	316	13
	C	90	185	296	12
	B + T6	...	440	507	13
	C + T6	...	461	520	16

(a) A, as received; B, after forming by internal pressure method; C, after forming by conventional method

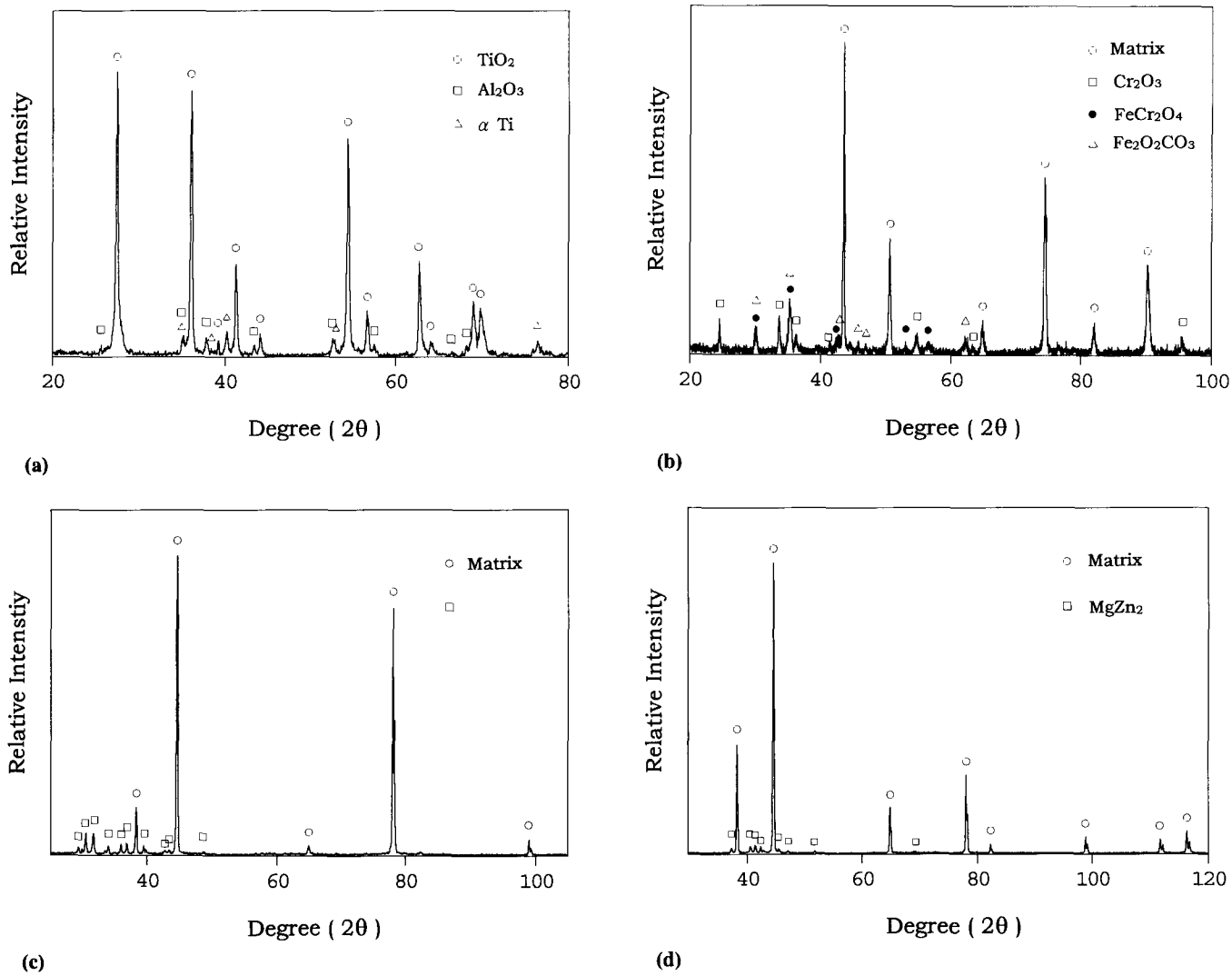

Fig. 13 XRD analysis on alloy surfaces. (a) Ti-6Al-4V formed with internal pressure at 927 °C for 30 min. (b) Superdux 64 stainless steel formed with internal pressure at 985 °C for 30 min. (c) 8090 Al-Li alloy formed with internal pressure at 485 °C for 30 min. (d) 7475 Al-Zn-Mg alloy formed with internal pressure at 500 °C for 30 min

Figure 11(a) shows the forming dome heights for 7475 Al-Zn-Mg alloy. The forming speed of this method is also close to that of argon blowing following the same pressure history (Fig. 11b) during formation. The wall thickness distributions of the dome-shaped specimen formed with internal pressure and argon are shown in Fig. 12.

The postforming tensile properties for the four alloys are given in Table 4, which lists results for both internal pressure

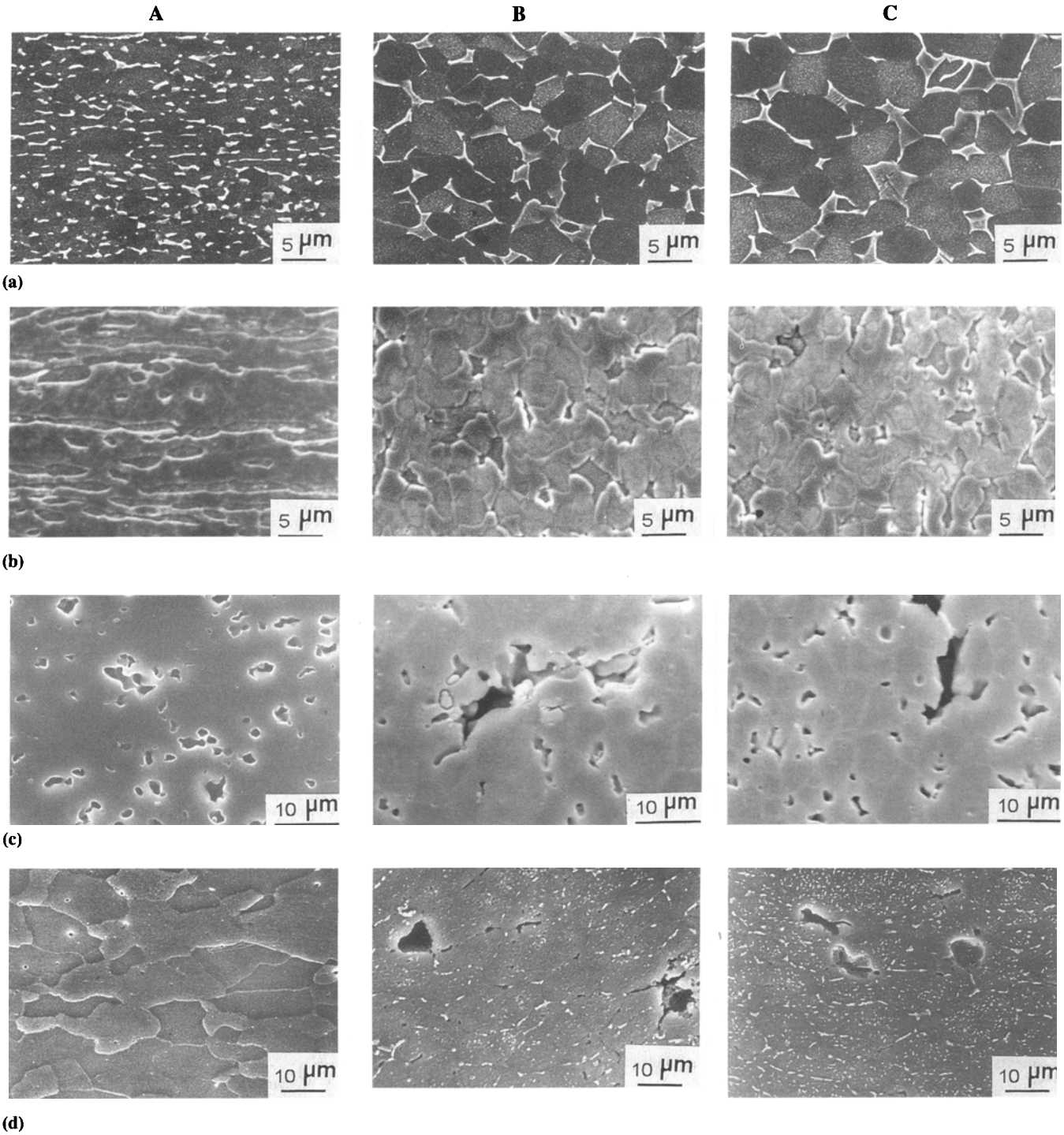

Fig. 14 Comparison of microstructures before and after forming. A, as received; B, after forming by internal pressure method; C, after forming by the conventional argon blowing method. (a) Ti-6Al-4V: 927 °C for 30 min; samples were etched with 2 mL HF + 5 mL HNO_3 + 100 mL H_2O. (b) Superdux 64 stainless steel: 985 °C for 30 min; samples were etched with 15 mL HCl + 5 mL HNO_3. (c) 8090 Al-Li: 485 °C for 15 min; samples were etched with 1 mL HF + 1.5 mL HCl + 10 mL HNO_3 + 87.5 mL H_2O. (d) 7475 Al-Zn-Mg: 500 °C for 20 min; samples were etched with 1 mL HF + 1.5 mL HCl + 10 mL HNO_3 + 87.5 mL H_2O

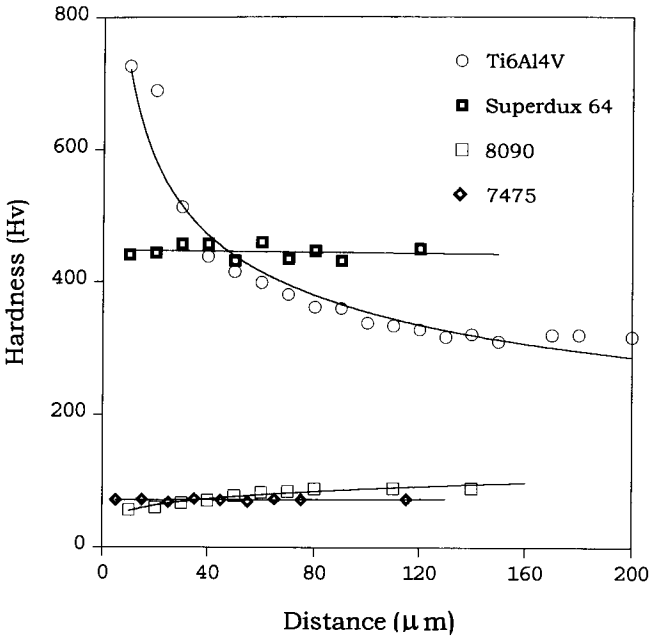

Fig. 15 Microhardness on the cross section of the plates formed with internal pressure. Ti-6Al-4V: 927 °C for 10 min. Superdux 64 stainless steel: 985 °C for 30 min. 8090 Al-Li: 485 °C for 15 min. 7475 Al-Zn-Mg: 500 °C for 20 min

forming and argon blowing. The effect of the superplastic strain (EST = 80) was to somewhat reduce the 0.2% proof stress (0.2PS), tensile stress (TS), and elongation of Ti-6Al-4V (Ref 9, 10). For Superdux 64 stainless steel, ductility was greatly reduced. The two aluminum alloys lost strength after superplastic forming (Ref 11, 12), but T6 heat treatment could lead to recovery of most of the 0.2PS and TS for both 8090 and 7475 alloys. In general, the 0.2PS, TS, and elongation values of the internal pressure forming method are smaller than those of argon blowing, except for Superdux 64, but the difference is small.

After internal pressure forming, some corrosion product is formed on the alloy surface. X-ray diffraction analysis revealed that TiO_2 rutile and αAl_2O_3 formed (Ref 13-15) on the surface of Ti-6Al-4V (Fig. 13a). For Superdux 64 stainless steel, the surface products were Cr_2O_3, $FeCr_2O_4$, and $Fe_2O_2CO_3$ (Fig. 13b). For 8090 Al-Li alloy, the major surface product was Li_2CO_3 (Ref 16, 17) (Fig. 13c), and for 7475 Al-Zn-Mg alloy, the surface product was $MgZn_2$ (Fig. 13d).

The microstructures of the four alloys before and after formation using this method and the conventional argon gas blowing method are shown in Fig. 14. The grain shape became more equiaxed, and the grains grew in size after formation (Ref 18). Comparison of the four alloys reveals no significant difference in microstructures between this method and the argon blowing method under similar forming conditions.

Figure 15 shows the microhardness depth profiles on the cross section of the plates for the four alloys (the origin is the interface of metal and oxide). It can be seen that Ti-6Al-4V was hardened by the solid solution of oxygen near the specimen surface (Ref 19, 20). In contrast, due to the depletion of lithium (Ref 21, 22), 8090 Al-Li alloy lost some hardness near the surface. For Superdux 64 stainless steel and 7475 Al-Zn-Mg alloy, their hardness showed no significant differences between the matrix and the region near the surface after internal pressure forming.

5. Conclusions

An innovative method using internal pressure has been applied for superplastic forming. In order to confirm the applicability of this method, the total pressures for decomposition of ($CaCO_3$ + C) and $MgCO_3$ have been theoretically calculated and experimentally measured. Furthermore, by using these powders, dome-shaped specimens of Ti-6Al-4V, Superdux 64 stainless steel, type 8090 alloy, and type 7475 alloy were produced. The surface products on the four alloys were examined and alloy microhardness was measured after formation. By comparing the forming speeds, wall thickness distributions, postforming tensile properties, and microstructures of the four alloys, the results of both internal pressure forming and argon forming were found to be similar.

Acknowledgment

This research was supported by the National Science Council, Taiwan, R.O.C., under contract No. NSC 83-0416-E-002-004.

References

1. J.M. Story, in *Superplasticity in Aerospace II*, T.R. McNelley and H.C. Heikkenen, Ed., Minerals, Metals, and Materials Society, 1990, p 151-166
2. W. Johnson, T.Y.M. Al-Naib, and D.L. Duncan, *J. Inst. Met.*, Vol 100, 1972, p 45
3. C.H. Hamilton and L.A. Ascani, Jr., Method for Superplastic Forming of Metals with Concurrent Diffusion Bonding, U.S. Patent 3,920,175, 1975
4. E.D. Weisert and G.W. Stacher, *Met. Prog.*, March 1977, p 33-37
5. K.F. Sahm and R. Holbein, Verfabren zur Herstellung von intergraeen Blechbauteileu aus hochfesten Aluminium Legieruugen, German Patent DE 3601868 A1, 1987
6. W. Bunk and H. Kellerer, Neue Fertizungsverfahrtn zue Verbesserung der Wirtschaftlichkeit, *Energie Wirtschaftlich Einsetzen*, Alumiun Verlag, Dusseldorf, 1984, p 138-150 (in German)
7. D.R. Gaskell, *Introduction to Metallurgical Thermodynamic*, 2nd ed., Hemisphere Publishing, 1981, Appendix A, p 585-586
8. L.B. Duffy, J.B. Hawkyard, and N. Ridley, *Mater. Sci. Technol.*, Vol 4, 1988, p 707-712
9. D.S. McDarmaid, A.W. Bowen, and P.G. Partridge, *Met. Sci. Eng.*, Vol 65, 1984, p 105-111
10. M.T. Cope, D.R. Evetts, and N. Ridley, *Mater. Sci. Technol.*, Vol 3, 1987, p 455-461
11. D.S. McDarmaid, P.G. Partridge, and A. Wisbey, in *Superplasticity in Advanced Materials*, S. Hori, M. Tokizane, and N. Furushiro, Ed., Japan Society for Research on Superplasticity, 1991, p 621-623

12. S.J. Hales and J.E. Lippard, *J. Mater. Eng. Perform.*, Vol 3 (No. 3), 1994, p 334-343
13. F. Motte, C. Coddet, P. Sarrazin, M. Azzopardi, and J. Besson, *Oxid. Met.*, Vol 10 (No. 2), 1967, p 113-127
14. I.A. Menzies and K.N. Strafford, *Corros. Sci.*, Vol 7, 1967, p 23-38
15. P. Kofstad, P.B. Anderson, and O.J. Krudtaa, *J. Less-Common Met.*, Vol 3, 1961, p 89-97
16. R.C. Dickinson, K.R. Lawless, and E. Wefers, *Scr. Metall.*, Vol 22, 1988, p 917-922
17. P. Holdway and A.W. Bowen, *J. Mater. Sci.*, Vol 24, 1989, p 2765-2774
18. A.K. Ghosh and C.H. Hamilton, *Metall. Trans. A*, Vol 13A, 1982, p 733-743
19. I.A. Menzies and K.N. Strafford, *J. Less-Common Met.*, Vol 12, 1967, p 85-106
20. A.I. Kahreci and G.E. Welsch, *Scr. Metall.*, Vol 22, 1986, p 1287-1290
21. P.G. Partridge, *Int. Mater. Rev.*, Vol 35 (No. 1), 1990, p 37-58
22. M. Ahmad, *Metall Trans. A*, Vol 18A, 1987, p 681-689